

## Spin relaxation by slow bulk motion in gypsum

E. Dumont, J. Jeener, and P. Broekaert

*Université Libre de Bruxelles, CPI-232, Boulevard du Triomphe, B-1040 Bruxelles, Belgium*

(Received 22 April 1993)

Using the techniques of spin thermodynamics in solids, we extended the theory of spin relaxation by slow bulk motion proposed by J. Jeener *et al.* [Adv. Magn. Reson. 14, 95 (1990)] to the more complex spectroscopic situation prevailing in gypsum in “2-lines” orientation. In order to test the calculations, we measured the additional rate of relaxation due to low-amplitude, low-frequency (1 KHz) rotational vibration of the whole crystal around various directions. In agreement with calculated predictions, we observed that the additional relaxation only affects the intermolecular spin-spin order at a rate which is temperature independent and proportional to the (average) square of the angular velocity of bulk rotation. The measured additional rate of relaxation also depends strongly on the orientation of the axis of rotation, in quantitative agreement with the calculated values.

## I. INTRODUCTION

The method for predicting relaxation rates in solid state NMR assumes that the spin Hamiltonian can be written as  $H(t) = H_0 + V(t)$ . The perturbing term  $V(t)$  causes a slow evolution of the quasi-invariants toward their equilibrium values. For the perturbative expansion of  $\rho(t)$  to converge,  $V(t)$  must have a correlation time much shorter than the time required by the system to reach a state of internal quasiequilibrium. However, there exist other tractable situations: infrequent atomic jumps,<sup>1,2</sup> slow continuous (possibly Brownian) rotation of the whole crystal.<sup>2-5</sup>

A new scheme, based on the formal solution of the Von Neumann equation, was developed by Jeener *et al.*<sup>2,4</sup> to predict the rate of relaxation of the spin-spin coupling energy for evolutions which remain close to thermodynamic adiabaticity. Theoretical predictions of the relaxation rates were made for slow but smooth evolution of the Hamiltonian, for infrequent jumps, and for a “wandering” Hamiltonian. Experimental confirmations of the predicted relaxation by quasiadiabatic variation of the Hamiltonian were obtained for crystalline  $\text{CaF}_2$  undergoing a slow continuous rotation<sup>2,4</sup> and also for rotational Brownian motion.<sup>5</sup> From a spin thermodynamic point of view,  $\text{CaF}_2$  is a system characterized by only two independent quasi-invariants of the motion: the Zeeman and dipolar energies. The good agreement between the theory and the experiment for  $\text{CaF}_2$  suggested extending the approach to a spin system with more complicated thermodynamic properties such as protons in a single crystal of gypsum.

From the NMR point of view, gypsum can be seen as a set of pairs of spins with a strong coupling within each pair and a much weaker coupling between pairs.<sup>6,8,9</sup> As the proton pairs in the crystal have two orientations only, the spectrum consists of two pairs of lines. For one particular orientation of the sample with respect to the large external magnetic field (henceforth called “2-

lines” orientation), all the molecules are spectroscopically equivalent (giving a characteristic Pake doublet absorption spectrum<sup>10</sup>) and the separation between the two lines of the absorption spectrum is maximum. Eisendrath *et al.*<sup>8,9</sup> have shown that, at the “2-lines” orientation of the sample, the evolution of the system toward thermal equilibrium can be described by four quasi-invariants of the motion: the Zeeman, intramolecular and intermolecular energies, and the population of the single pair singlet.

To test the new scheme in a nontrivial experimental setting, we submitted the sample, in a controlled manner, to a slow bulk rotation, of small amplitude ( $< 1^\circ$ ), on either side of the “2-lines” orientation. The rotation had to be of low amplitude around the “2-lines” orientation for the description of the spin thermodynamics with four quasi-invariants to remain suitable. The “2-lines” orientation corresponds to an orientation of the sample such that the external magnetic field is parallel to the  $\mathbf{b}$  axis in the Atoji unit cell.<sup>16,17</sup> The time dependence of the Hamiltonian induced by the rotation had to be slow compared to the characteristic time of the process leading to an internal equilibrium of the spin system.

The theory of relaxation or saturation by quasiadiabatic variation of the Hamiltonian applied to the model of gypsum undergoing a slow vibration in rotation led to the prediction of an additional, fast, temperature independent, relaxation (more exactly saturation) mechanism acting on the quasi-invariant intermolecular energy only. The present paper describes the predictions and the experimental confirmation of this relaxation mechanism.

## II. THEORETICAL CONTEXT: EFFECTIVE HAMILTONIAN

The Hamiltonian of the spin system immersed in a large external magnetic field, in slow motion around the “2-lines” orientation, can be written as<sup>8,9</sup>

$$H(t) = H_{Zee} + H_M(t) + H_I(t), \quad (2.1)$$

where  $H_{Zee}$ ,  $H_M(t)$ , and  $H_I(t)$  denote, respectively, the Zeeman, intramolecular, and intermolecular Hamiltonian. The evolution of the spin system in a high magnetic field is adequately described, on the time scale of our experiments, by Hamiltonian (2.1) in which the parts of  $H_M(t)$  and  $H_I(t)$ , which are nonsecular with respect to  $H_{Zee}$ , are neglected.<sup>6,8,9</sup>

Eisendrath *et al.*<sup>8,9</sup> have shown that the spin system can be seen as an assembly of proton pairs with a weak coupling between pairs. The Hamiltonian of such spin system can be written as

$$H(t) = H_{\text{mol}}(t) + H_{\text{inter}}(t), \quad (2.2)$$

with

$$H_{\text{mol}}(t) = H_{Zee} + H_M^{\text{secular}/H_{Zee}}(t) = \sum_{i=1}^{N_{\text{mol}}} H_{\text{mol}}^i(t) \quad (2.3)$$

and

$$H_{\text{inter}}(t) = H_I^{\text{secular}/H_{Zee}}(t) = \sum_{i=1}^{N_{\text{mol}}} \sum_{j>i}^{N_{\text{mol}}} H_{\text{inter}}^{ij}(t), \quad (2.4)$$

where  $N_{\text{mol}}$  is the number of molecules in the sample and secular/ $H_{Zee}$  means "secular with respect to  $H_{Zee}$ ."

By analogy with the treatment of a system with Zeeman and dipolar order only, we will consider  $H_{\text{mol}}(t)$  as an unperturbed Hamiltonian (with unequally spaced energy levels) while the "small" perturbing term  $H_{\text{inter}}(t)$  is playing a role similar to the dipolar Hamiltonian.<sup>6</sup> We can further pursue the analogy by neglecting the part of  $H_{\text{inter}}(t)$  not secular with respect to  $H_{\text{mol}}(t)$ . This restricts our calculations to those orientations in which the splitting of the two absorption lines is much larger than the width of each line and neglects the possible overlap of these lines. The main justification for such an approximation is the good agreement between theoretical predictions and the experimental results.<sup>8,9</sup> Thus

$$H'_{\text{inter}}(t) = H_I^{\text{secular}/H_{\text{mol}}(t)}(t). \quad (2.5)$$

In the temperature range in which the experiments were performed, the water molecules caged in the lattice undergo rapid thermally activated flips that exchange the position of the two hydrogen atoms. These permutations of the protons modify only the intermolecular energy. The average time between two flips ( $\approx 10^{-7}$  s) is much smaller than the time required by the spin system to reach a state of internal quasiequilibrium (which is on the order of  $T_2$  or  $\approx 10^{-4}$  s in studied samples), the effective Hamiltonian describing the evolution of this spin system is an average over the possible permutations of the protons.

In the course of the small oscillatory rotation of the sample around the "2-lines" orientation, the effective intramolecular Hamiltonian does not remain identical for all the molecules of the sample. That is, if we label the molecules so that the even molecules correspond to one orientation and the odd to the other, then  $H_{\text{mol}}^{i(\text{odd})}(t)$

is generally not equal to  $H_{\text{mol}}^{j(\text{even})}(t)$  except at the time the sample crosses the exact "2-lines" orientation. This suggests<sup>7</sup> writing the effective Hamiltonian,  $[H_{\text{eff}}(t) = H_0(t) + H_1(t)]$  as a sum of two terms. The first term being identical for all the molecules, throughout the motion of the sample :

$$H_0(t) = H_{Zee} + \overline{H}_M^{\text{secular}/H_{Zee}}(t), \quad (2.6)$$

where  $\overline{H}_M^{\text{secular}/H_{Zee}}(t)$  is the average of the intramolecular Hamiltonian over the two possible orientations of the water molecules, and a second term which includes the intermolecular Hamiltonian and the small deviation from the "average" molecular Hamiltonian:

$$H_1(t) = \left( H_M^{\text{secular}/H_{Zee}}(t) - \overline{H}_M^{\text{secular}/H_{Zee}}(t) \right) + H_I^{\text{secular}/H_{\text{mol}}(t)}(t). \quad (2.7)$$

$H_0(t)$  can be written as

$$H_0(t) = \sum_{\alpha=1}^4 E_{\alpha}(t) \sum_{i=1}^{N_{\text{mol}}} |i, \alpha\rangle \langle i, \alpha| = \sum_{\alpha=1}^4 E_{\alpha}(t) N^{\alpha}, \quad (2.8)$$

where  $\alpha$  labels the four eigenstates of the single-molecule Hamiltonian  $H_0^i$ , with eigenvalues  $E_{\alpha}$ . The symbol  $N^{\alpha}$  is the occupation number operator for the molecular state  $\alpha$ .<sup>6</sup> The small rotation of the sample in the external magnetic field will cause a small time evolution of  $E_{\alpha}$ , but not of the  $N^{\alpha}$ , hence these rotations will not change the average values of the invariants built upon the  $N^{\alpha}$ ; i.e., the Zeeman and intramolecular energies and the population of the singlet state.

We get rid of  $H_0(t)$  in the equation of the motion of the density operator of the spin system, by a transformation defined by

$$\tilde{A}(t) = Q^{\dagger}(t) A(t) Q(t), \quad (2.9)$$

with

$$i\hbar \frac{d}{dt} Q(t) = H_0(t) Q(t) \quad (2.10)$$

and the initial condition  $Q(t_0) = 1$ . The equation of the motion of the density operator describing the spin system becomes

$$i\hbar \frac{d}{dt} \tilde{\rho}(t) = [\tilde{H}_1(t), \tilde{\rho}(t)]. \quad (2.11)$$

As  $[H_0(t_1), H_0(t_1)] = 0$  for any  $t_1$  and  $t_1$  in the interval of interest, Eq. (2.11) becomes

$$i\hbar \frac{d}{dt} \tilde{\rho}(t) = [H_1(t), \tilde{\rho}(t)]. \quad (2.12)$$

We can then use the method developed by Jeener *et al.*<sup>2</sup> to express the rate of saturation of the intermolecular energy by slow bulk rotation as a function only of  $\tilde{H}_1(t_0)$  and  $\left. \frac{d}{dt} \tilde{H}_1(t) \right|_{t_0}$ , where

$$\hat{H}_1(t) = H_1(t) \left[ \frac{\text{Tr}\{1\}}{\text{Tr}\{[H_1(t)]^2\}} \right]^{\frac{1}{2}} \quad (2.13)$$

is a dimensionless, normalized version of the effective intermolecular Hamiltonian.

Consequently

$$\frac{d}{dt} \langle \hat{H}_1(t) \rangle = -R_{\text{smooth}} \langle \hat{H}_1(t) \rangle, \quad (2.14)$$

with

$$R_{\text{smooth}} = \frac{\frac{1}{2} \sqrt{\pi} K \text{Tr} \left\{ \left[ \frac{d}{dt_0} \hat{H}_1(t_0) \right]^2 \right\}}{\text{Tr}\{1\}} \quad (2.15)$$

and

$$K^2 = \frac{2\hbar \text{Tr} \left\{ \left[ \frac{d}{dt_0} \hat{H}_1(t_0) \right]^2 \right\}}{\text{Tr} \left\{ -[H_1(t_0), \frac{d}{dt_0} \hat{H}_1(t_0)]^2 \right\}}. \quad (2.16)$$

When the sample is submitted to a vibration in rotation,  $\frac{d}{dt} \hat{H}_1(t)|_{t_0}$  is proportional to  $\omega$ , the instantaneous angular velocity of rotation. Hence  $R_{\text{smooth}}$ , averaged over long time intervals (as measured in a realistic experiment), is proportional to the mean squared angular velocity of the sample  $\langle \omega^2 \rangle$ . Experimentally, the observed relaxation rate is the sum of  $R_{\text{smooth}}$  and  $R_{\text{SL}}$  (rate of relaxation measured without vibrations in rotation). Thus

$$\frac{d}{dt} \langle \hat{H}_1(t) \rangle = (R_{\text{smooth}} + R_{\text{SL}}) \langle \hat{H}_1(t) \rangle. \quad (2.17)$$

Our predictions can be summarized as follows.

(1) The motion in rotation of the sample affects only the intermolecular orders.

(2) The predicted relaxation rate,  $R_{\text{smooth}}$ , is independent of temperature.

(3)  $R_{\text{smooth}}$  is proportional to  $\langle \omega^2 \rangle$ .

(4)  $R_{\text{smooth}}$  depends on the orientation of the axis of rotational vibration with respect to the crystal axis of the sample.

The numerical evaluation of  $R_{\text{smooth}}$  from Eq. (2.15) involves the following steps: first we have to express  $\hat{H}_1(t_0)$  in terms of  $H_1(t_0)$  as given in Eq. (2.7). The traces over all the states of the spin system can then be reduced to sums over all the molecules of the crystal, of terms depending solely on the geometric properties of the lattice. The traces of  $[H(t_0)]^2$ ,  $\left[ \frac{d}{dt_0} H(t_0) \right]^2$ , and  $H(t_0) \frac{d}{dt_0} H(t_0)$  involve sums over pairs of molecules whereas the trace of  $\left[ H(t_0), \frac{d}{dt_0} H(t_0) \right]^2$  involves a sum over three molecules. The individual terms of the summations decrease very rapidly with the distance between spins so that sums over all pairs and combinations of three molecules within a sphere of radius 1.5 nm (226 pairs and 50 850 combinations of three molecules) gave satisfactory results. We performed calculations in which

the axis of vibration was varied with respect to the crystal axis in the **ac** plane and the magnetic field was aligned along the **b** axis in the Atoji unit cell.<sup>16,17</sup>

### III. MATERIAL AND METHODS

#### A. Experimental setup

To vibrate the sample in rotation, we secured it to the lower end of a glass tube oscillating in its high- $Q$  fundamental torsional mode. We checked experimentally that a small static change in orientation ( $< 1^\circ$ ) did not change significantly the relaxation rates of the various invariants or the shape and amplitude of the FID signals. The experiments were performed at a NMR frequency of 30 MHz.

#### B. Decomposition of the dipolar signal into its intra- and intermolecular components

The only information directly accessible through pulse experiments are the Zeeman and the dipolar FID signals. The dipolar FID signal  $S_D(t)$  consists of a superposition of a signal proportional to intramolecular order,  $MS_M(t)$ , and a signal proportional to intermolecular order,  $IS_I(t)$ . Thus

$$S_D(t) = MS_M(t) + IS_I(t). \quad (3.1)$$

The weights ( $M$  and  $I$ ) associated with  $S_M(t)$  and  $S_I(t)$  are the amounts of intra- and intermolecular order, respectively. To observe the relaxation of these quasi-invariants we have to measure the amounts order  $M$  and  $I$  for various time delays ( $\tau_1$  in Fig. 2) between the preparation of the spin system into a specific thermodynamics state and the observation of the dipolar FID signal. The problem is linear and easily solved if one knows beforehand the shape of the FID signals associated with intra- and intermolecular order [ $S_M(t)$  and  $S_I(t)$ , respectively].

The absorption spectrum corresponding to Zeeman order  $[\chi''_Z(\omega)]$  appears as a superposition of two lines<sup>8-10</sup> (the Pake doublet), described, respectively, by  $F(\omega - \omega_m)$  and  $F(\omega + \omega_m)$  as shown by Fig. 1(a). The separation between those two lines is due to the intramolecular coupling whereas the broadening of the lines is attributed to the intermolecular coupling. The intramolecular spectrum  $[\chi''_M(\omega)]$  is simply the Zeeman spectrum with one line in emission rather than in absorption [Fig. 1(b)]. For crystal orientations for which the Zeeman spectrum consists of a single line  $F(\omega)$ , centered on  $\omega = 0$ , the presence of intermolecular order manifests itself by an absorption spectrum of the type  $\omega \cdot F(\omega)$  which is emissive on one side of the line and absorptive on the other side, following the usual pattern for dipolar order in solids. When the two components of the Pake doublet are well separated, the presence of intermolecular order manifests itself separately on each component [Fig. 1(c)]. Hence the Zeeman, the intramolecular, and the intermolecular absorption spectra are given, respectively, by

$$F(\omega + \omega_m) + F(\omega - \omega_m), \quad (3.2a)$$

$$F(\omega + \omega_m) - F(\omega - \omega_m), \quad (3.2b)$$

and

$$(\omega - \omega_m)F(\omega - \omega_m) + (\omega + \omega_m)F(\omega + \omega_m), \quad (3.2c)$$

where  $2\omega_m$  is the line separation due to intramolecular coupling.

Abraham<sup>11</sup> has shown that the shape of a FID signal, in a frame rotating at the frequency of the center of the line, corresponding to Zeeman order in  $\text{CaF}_2$  (which has a typical one-line absorption spectrum), can be very well approximated by

$$f_{Z,1 \text{ line}}(t) = a \exp(b^2 t^2) \sin(ct) / (ct). \quad (3.3)$$

$f_{Z,1 \text{ line}}(t)$  is thus an analytical approximation to the real part of the Fourier transform of  $F(\omega)$ .

Assuming that each component [ $F(\omega - \omega_m)$  and  $F(\omega + \omega_m)$ ] of the gypsum protons spectrum can be approximated by the Fourier transform of  $f_{Z,1 \text{ line}}(t)$  (with frequency shifts of  $-\omega_m$  and  $+\omega_m$ , respectively) and using the relations linking the absorption spectra corresponding to Zeeman, intramolecular, and intermolecular order [cf. Eqs. (3.2)], it is possible to construct satisfactory analytical descriptions of the shapes of the Zeeman, intra-, and intermolecular FID signals [cf.  $f_Z(t)$ ,  $f_M(t)$ , and  $f_I(t)$  in Fig. 3]. The parameters  $b$  and  $c$  in Eq. (3.3) and

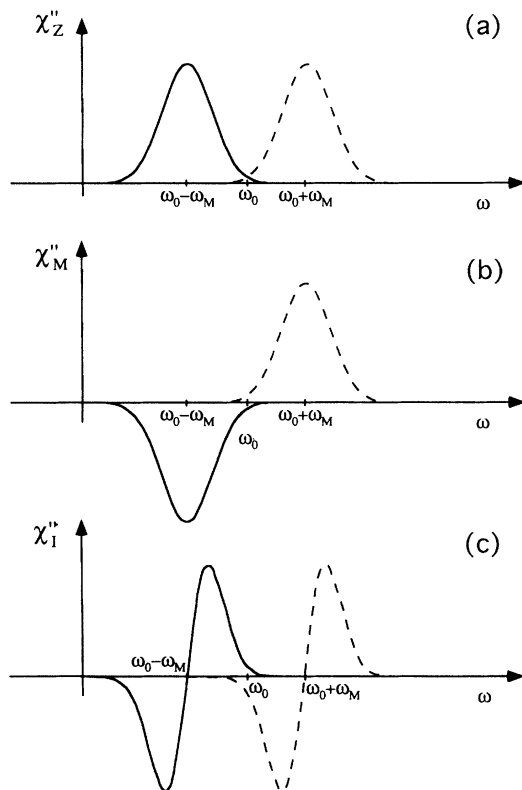


FIG. 1. Schematic absorption spectra corresponding to Zeeman order (a), intramolecular order (b), and intermolecular order (c).

the line separation  $2\omega_m$  were adjusted by a least squares fit to the observed Zeeman FID signal.

### C. Pulse sequence

Dipolar order at room temperature does not give rise to any conveniently observable signal unless the spin system is previously prepared in a state of high dipolar order. It is possible, by pulse method, to transfer Zeeman order selectively into mostly intramolecular or mostly intermolecular order. This technique, developed by Jeener and Broekaert,<sup>13,14</sup> consists of applying two pulses separated by a delay  $\tau_0$  and with the phase of the second pulse shifted by  $90^\circ$ . The transfer of order from Zeeman to dipolar is maximum (for a system with one spin species) when the first pulse is a  $90^\circ$  pulse and the second is a  $45^\circ$  pulse. The time delay  $\tau_0$  (cf. Fig. 2) is of fundamental importance since it controls the amount of intramolecular and intermolecular order prepared. It has been shown<sup>13</sup> that the efficiency of transfer of Zeeman order into intramolecular or intermolecular order as a function of  $\tau_0$  is proportional to  $S_M(\tau_0)$  and  $S_I(\tau_0)$ , respectively, where  $S_M(\tau_0)$  and  $S_I(\tau_0)$  are the amplitudes observed at time  $\tau_0$  of the intra- and intermolecular FID signals. Further treatment of the experimental results requires the acquisition of a reference Zeeman signal obtained under the same experimental conditions as the dipolar signal. To avoid the problem of base line determination, we also alternated reading pulses along  $X$  and  $-X$  and subtracted the signals so obtained. The comb of saturating  $90^\circ$  pulses was used to ensure that the initial thermodynamic state of the system was always identical without having to wait for the system to return to complete equilibrium with the lattice. The singlet population, however, is left unaffected by rf pulses. Nevertheless the cross relaxation through dipolar coupling between singlet population and intramolecular order is such a slow process that we expected the effect of an excess singlet population on the intramolecular order to be negligible.<sup>8,9</sup>

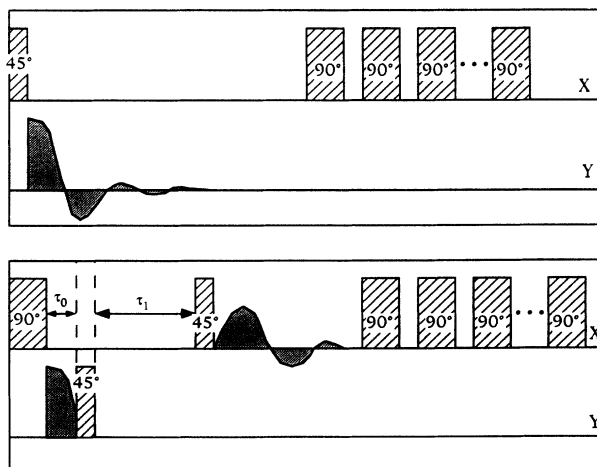


FIG. 2. The pulse sequence.

### D. Data processing

The experimental signals were digitized and transferred to a computer in the form of vectors containing 512 points corresponding to a measurement of the FID for a total duration of 100  $\mu\text{s}$ . The signals are then corrected by software for linear detector imperfections and phase and frequency shifts using the method described in Ref. 15. The dipolar signal appears on the channel in phase with the  $45^\circ$  read pulse and the Zeeman signal appears on the other channel of the pairs of orthogonal detectors. The determination of the amounts of intra- and intermolecular order, up to a constant factor, is a two-step process. First, we perform a least squares adjustment<sup>12</sup> of  $f_Z(n)$  on the digitized experimental Zeeman signal  $S_Z(n)$  to determine the parameters necessary for the computation of  $f_M(n)$  and  $f_I(n)$ . Second, we determined the values of  $M$  and  $I$  by linear least squares adjustment<sup>12</sup> of  $Mf_M(n) + If_I(n)$  on the dipolar signal  $S_D(n)$  (see Fig. 3). The advantage of working on the FID signals is that only the part of the signal which has a good signal-to-noise ratio is taken into account (the beginning of the signal is usually distorted by the remnants from the large rf pulse). To determine the optimal delay  $\tau_0$  to prepare selectively mostly intramolecular or mostly intermolecular order, we observed the efficiency of transfer of Zeeman order into intra- and intermolecular order as a function of  $\tau_0$ .

Figure 4 shows the results of an experiment in which  $\tau_0$  was varied from 1 to 80  $\mu\text{s}$ . The resulting dipolar signals were then interpreted as a superposition of  $f_M(n)$  and  $f_I(n)$ . The calculated weights  $M$  and  $I$  were plotted as a function of  $\tau_0$ . It appears that for  $\tau_0 = 10 \mu\text{s}$  the transfer of order is from Zeeman to intramolecular order only, whereas a delay  $\tau_0$  of 20  $\mu\text{s}$  produces almost exclusively intermolecular order.

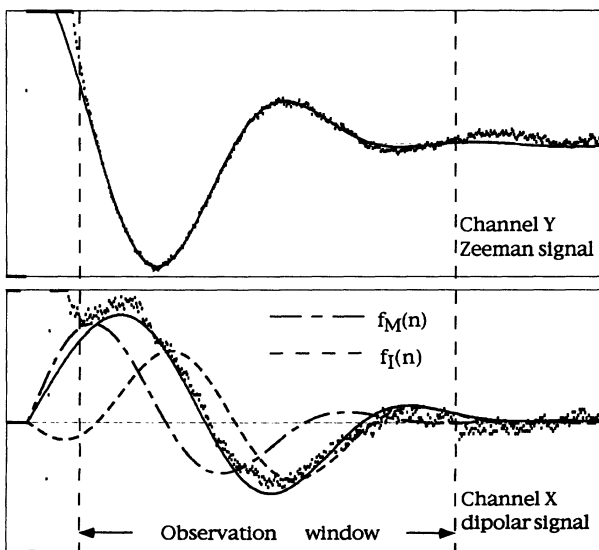


FIG. 3. Top: the Zeeman signal,  $S_Z(n)$  with the adjusted function  $f_Z(n)$ . Bottom: the dipolar signal with the adjusted functions  $f_M(n)$ ,  $f_I(n)$ , and  $Mf_M(n) + If_I(n)$ .

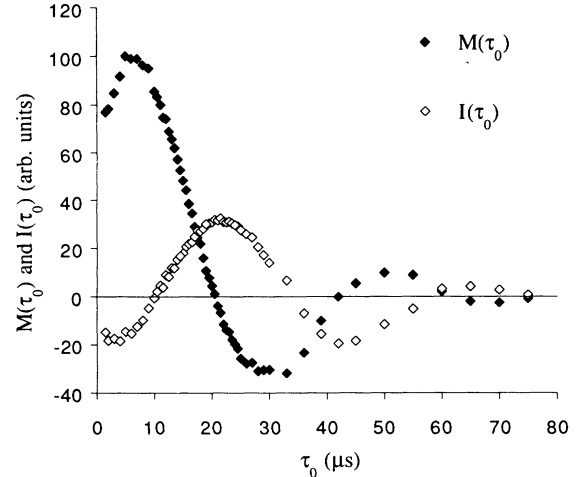


FIG. 4. Amounts of intra- and intermolecular order obtained as a function of the delay between the preparation pulses:  $M(\tau_0)$  and  $I(\tau_0)$ . [The efficiency of transfer is proportional to  $S_M(\tau_0)$  and  $S_I(\tau_0)$ .]

## IV. RESULTS

### A. Relaxation of the intra- and intermolecular order with and without vibration

The theory of saturation by quasiadiabatic variation of the Hamiltonian applied to the complex spin thermodynamics of gypsum led to the prediction that only intermolecular order would be affected by the bulk vibration in rotation of the crystal. To test this prediction we measured the relaxation rate of the intra- and intermolecular order with and without vibration. Figures 5 and 6 show that intramolecular order relaxes at the same rate with or without vibration whereas the intermolecular order saturates more rapidly in the presence of vibration. We

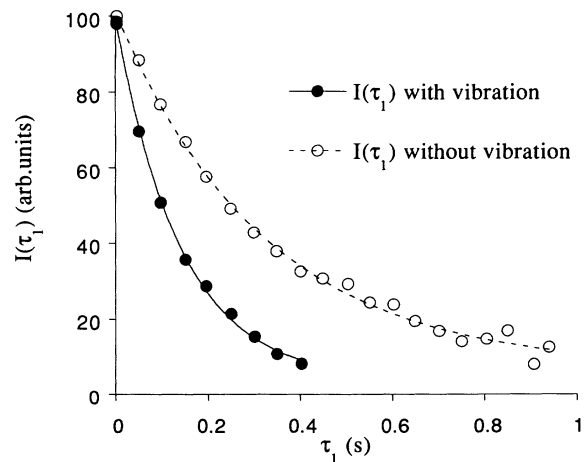


FIG. 5. Intermolecular order as a function of  $\tau_1$ , the delay between preparation and observation, with and without vibrations of the sample, after a preparation of essentially intermolecular order.

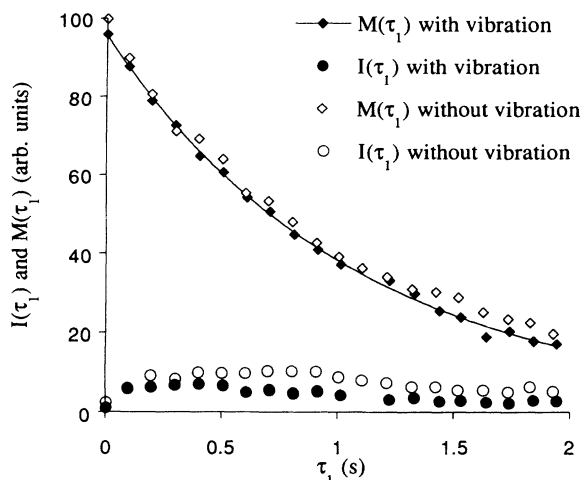


FIG. 6. Intra- and intermolecular order as a function of  $\tau_1$ , with and without vibrations of the sample, after a preparation of essentially intramolecular order.

performed these experiments at the highest possible temperature (above 348 K, the crystal rapidly loses its water molecules) to benefit from a larger difference between the intra- and intermolecular spin-lattice relaxation times. Moreover, the relaxation time of the intramolecular order is very long so that by monitoring the appearance of the intermolecular signal we can verify that cross relaxation between intra- and intermolecular energies is indeed slow on the time scale of the other relevant processes such as spin-lattice relaxation and saturation by slow vibrational rotation of the sample.

### B. The relaxation rate as a function of the amplitude of vibration

To observe the dependence of the rate of relaxation on the mean quadratic angular velocity of the crystal  $\langle \omega^2 \rangle$ , we varied the amplitude of vibration of the sample  $A_v$  (the frequency  $\nu$  was fixed by the vibrational mode of our glass tube). The amplitude of vibration was measured by reflection of light on a mirror fixed on the sample. Figure 7 shows the measurement of the relaxation rate of

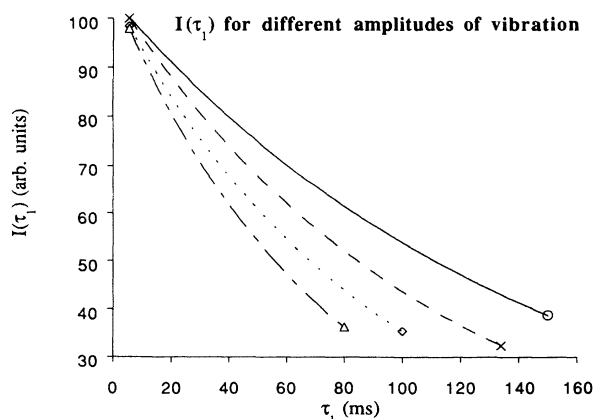


FIG. 7. Intermolecular order as a function of  $\tau_1$  for different amplitudes of vibration  $A_v$ .

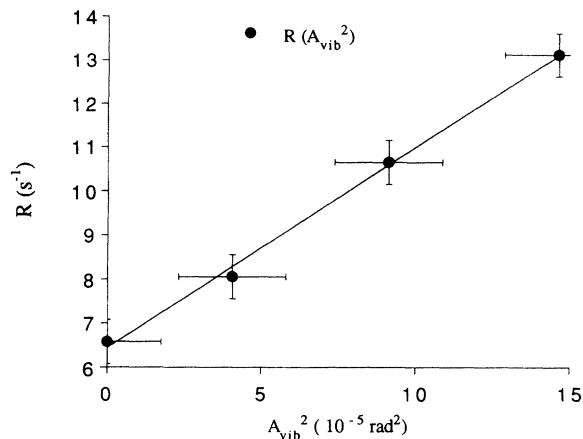


FIG. 8. Relaxation rate as a function of the square of the amplitude of vibration  $A_v^2$ .

the intermolecular order at four different amplitudes of vibration. A plot of the relaxation rates obtained above as a function of  $A_v^2$  confirms the linear dependency of  $R_{smooth}$  on  $\langle \omega^2 \rangle$ , see Fig. 8.

### C. The relaxation rate as a function of temperature

We measured the relaxation rate at temperatures from 303 to 348 K to check if the relaxation due to the rotational vibration of the sample is independent of the temperature. The graph of the relaxation rates  $R_M$ ,  $R_I$ , and  $R_{smooth}$  as a function of temperature summarizes the results obtained. We can see in Fig. 9 that although  $R_M$  and  $R_I$  vary significantly over the temperature range,  $R_{smooth}$  remains constant.

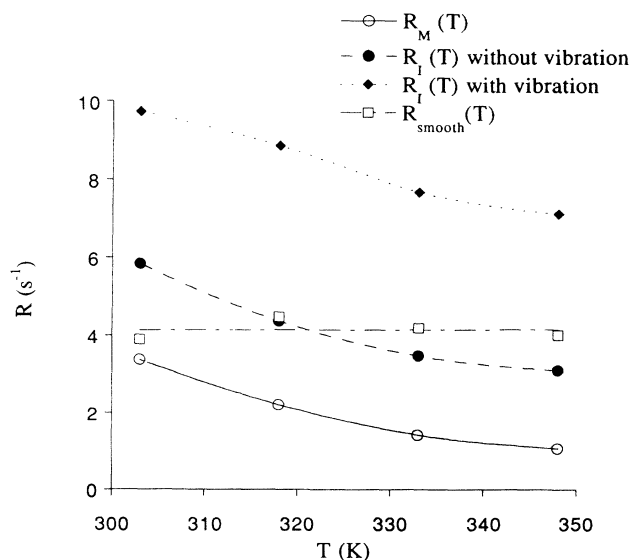


FIG. 9. Measurement of the relaxation rates  $R_M$ ,  $R_I$ , with and without vibration, and  $R_{smooth}$ , as a function of the temperature (the lines are just guides for the eyes).  $R_{smooth}$  is essentially independent from the temperature whereas both  $R_M$  and  $R_I$  vary significantly over the temperature range

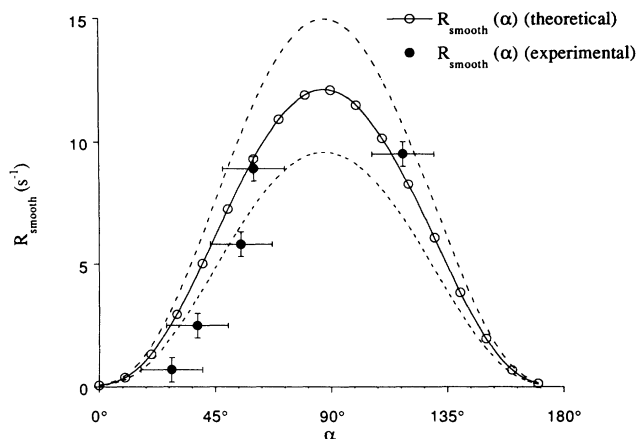


FIG. 10. Experimental data plotted against theoretical predictions. The uncertainty in the amplitude of vibration which translates into an upper and lower bound on the theoretical predictions is represented here as dashed curves.

#### D. Relaxation rate as a function of the orientation of the axis of vibration of the sample

The best test of the predictive value of the theory is the comparison between the experimental and the numerical rates for several orientations of the axis of vibration with respect to the crystal axis of the sample. Figure 10 shows on the one hand the numerical values represented here as a continuous function (but obtained by lattice sum for 18 distinct orientations of the axis of vibration relative to the crystal). We represent the uncertainty in the amplitude of vibration by the two dashed curves calculated for the extreme values of the amplitude of vibration. On the other hand the experimental points are displayed with error bars to account for the uncertainty in the determi-

nation of  $R$  ( $\Delta R = 0.4 \text{ s}^{-1}$ ) and the inaccuracy in the determination of the axis of vibration. The agreement between the predicted and observed behavior of  $R_{\text{smooth}}$  is very satisfactory and provides a clear test of the validity of the proposed extension of the theory of relaxation by quasiadiabatic evolution of the spin Hamiltonian.

#### V. CONCLUSION

The theory of relaxation by slow quasiadiabatic evolution of the Hamiltonian was extended to the spectroscopic situation prevailing in gypsum in the "2-lines" (of proton NMR) orientation. The following predictions were confirmed by experiments in which gypsum crystals were submitted to 1 KHz, low-amplitude, bulk rotational vibration: the additional relaxation only affects the intermolecular spin-spin order at a rate which is temperature independent and proportional to the (average) square of the angular velocity of bulk rotation. The measured additional rate of relaxation depends strongly on the orientation of the axis of rotation, in quantitative agreement with the calculated value.

#### ACKNOWLEDGMENTS

One of us (E.D.) is especially indebted to IRSIA (Institut pour l'Encouragement de la Recherche Scientifique dans l'Industrie et l'Agriculture), the Fondation Van Buren, and APMO for their financial support during this research. This research was also supported in part by FRSM (Fonds de la Recherche Scientifique Médicale-Loterie Nationale), crédit No. 9.4578.90, and the Communauté Française de Belgique, crédit A.R.C.-convention No. 91/96-149.

- <sup>1</sup> C. P. Slichter and D. Ailion, *Phys. Rev.* **135**, A1099 (1964).
- <sup>2</sup> J. Jeener, J. D. Bell, P. Broekaert, E. Dumond, and M. Koenig, *Adv. Magn. Reson.* **14**, 95 (1990).
- <sup>3</sup> J. F. J. M. Pourquié and R. A. Wind, *Phys. Lett.* **55A**, 347 (1965).
- <sup>4</sup> J. Jeener, J. D. Bell, P. Broekaert, P. Thomas, and E. Dumont (unpublished).
- <sup>5</sup> D. Esteve, C. Urbina, M. Goldman, H. Frisby, H. Raynaud, and L. Strzeleki, *Phys. Rev. Lett.* **52**, 1180 (1984).
- <sup>6</sup> J. Jeener, *Adv. Magn. Reson.* **3**, 205 (1968).
- <sup>7</sup> J. Jeener, *Adv. Magn. Reson.* **3**, 213 (1968).
- <sup>8</sup> H. Eisendrath, W. Stone, and J. Jeener, *Phys. Rev. B* **17**, 47 (1978).
- <sup>9</sup> H. Eisendrath and J. Jeener, *Phys. Rev. B* **17**, 54 (1978).

- <sup>10</sup> P. E. Pake, *J. Chem. Phys.* **16**, 327 (1948).
- <sup>11</sup> A. Abragam, *The Principles of Nuclear Magnetism* (Oxford University Press, London, 1961).
- <sup>12</sup> W. H. Press, B. P. Flannery, S. A. Teukolsky, and W. T. Vetterling, *Numerical Recipes, The Art of Scientific Computing* (Cambridge University Press, Cambridge, 1989).
- <sup>13</sup> J. Jeener and P. Broekaert, *Phys. Rev.* **157**, 232 (1967).
- <sup>14</sup> P. Broekaert and J. Jeener, *Phys. Rev. B* **15**, 4168 (1977).
- <sup>15</sup> J. Jeener and C. Segebarth, *Rev. Sci. Instrum.* **46**, 1478 (1975).
- <sup>16</sup> M. Atoji and R. E. Rundle, *J. Chem. Phys.* **29**, 1306 (1958).
- <sup>17</sup> W. F. Cole and C. J. Lancucki, *Acta Crystallogr. B* **30**, 921 (1974).

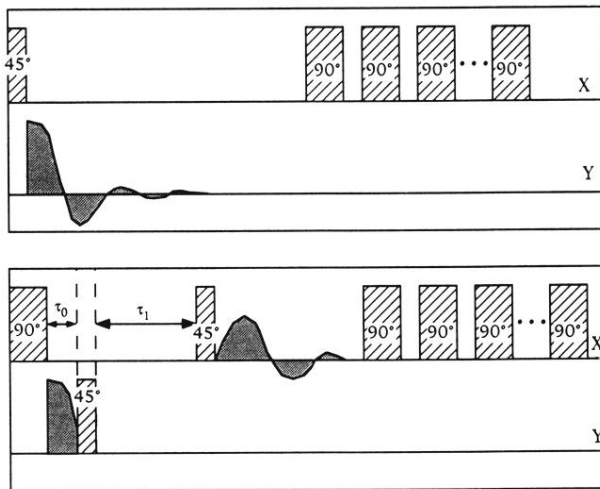


FIG. 2. The pulse sequence.